# ISLAMIC UNIVERSITY OF TECHNOLOGY

## ORGANIZATION OF ISLAMIC COOPERATION

# ENERGY HARVESTING FROM PZT-5A INTIGRATED BIMORPH CANTILEVER BEAM


**Prepared By-**

**Md. Al-Imran Khan (131455)**

**Abdullah Al Mamun (131457)**

**Supervised By-**

**Prof. Dr. Md. Zahid Hossain**

**Head,**
**Department of Mechanical and Chemical Engineering**
**Islamic University of Technology**
**Gazipur, Bangladesh.**

A Thesis Submitted to the Academic Faculty in Partial Fulfillment of the Requirements for the Degree of

**BACHELOR OF SCIENCE IN MECHANICAL ENGINEERING**

Department of Mechanical and Chemical Engineering (MCE)

Islamic University of Technology (IUT)

Approved by-

---

**Prof. Dr. Md.Zahid Hossain**

Supervisor and Head of the department ;

Mechanical and Chemical Engineering,(MCE)

Islamic University of Technology (IUT),

Boardbazar, Gazipur-1704.

Date: ……..

## Table of Contents

## List of Tables:



## List of Figures:

## Abstract

This paper presents a theoretical model for simulating a piezoelectric integrated bimorph cantilever beam which acts like a power harvester. A point mass is attached on the free end of the beam. Acceleration is applied in the base of the beam and that causes transvers vibration of the beam. Electric potential is generated on the beam surface. How much electric energy is generated, was simulated by comsol multiphysics. By changing various dimensions and parameters, how the output power varies, were studied.

# 1 Introduction:

Energy harvesting (also known as energy scavenging) is the energy conversion process by which electrical energy is harvested from various ambient energy sources (e.g., solar power, thermal energy, wind energy, noise, and vibration). Mechanical strain from machine vibration is one of the most available ambient energy sources easily found in civil structures, machines, or human bodies. Among the energy conversion principles to convert mechanical strain into electrical energy, piezoelectricity is known to be one of the most effective and practical ways [1]

With the increasing developments in the field of technology the use of wireless, remote system and micro electro mechanical systems technology is gradually increasing. There are some applications like micro planes, wireless sensors where these devices can be placed in a very remote locations such as embedded in some structural sensor or on a bridge or Global Positioning Systems (GPS) tracking devices on animals in the wild. But when the battery is exhausted or extinguished, the sensors must be retrieved and the battery should be replaced which is a very tedious work. So these devices should be given their own power supply. A self-contained renewable energy supply is incumbent for this purpose in the field of renewable energy harvesting has become a vital section [2]. Energy harvesting is the most effective way to the solution of gradually decreasing fossil fuels and furthermore it is also echo friendly and sustainable One of the energy harvesting is to convert mechanical strain into electrical energy. Mechanical strain is vastly found in machine vibration. Among the energy conversion principles to convert mechanical strain into electrical energy Piezoelectricity is known to be one of the most effective ways. By using piezoelectric material we can easily fulfill the demand of small electric power which is very essential in the modern era of science and technology [3]. With the increasing demand of micro materials which require very less amount of electrical power piezoelectric material is the most possible solution for these material. For this reason further development of piezoelectric material as well as piezoelectricity is a very common practice in the scientifically developed countries . Recently, the piezoelectric energy harvesters with unique structures and fabrication methods have been significantly developed, which can be classified with bulk type, micro electromechanical systems (MEMS), and flexible energy harvesters.

## 1.1 Background:

In March, 2010 Shudong Yu, Siyuan He and Wen Li published the paper “Theoretical and experimental studies of beam bimorph piezoelectric power harvester”. In that paper they described theoretical and experimental modeling of piezoelectric bimorph cantilever beam. They proposed a bimorph cantilever beam model (Integrated PZT-5A) with and without a point mass on free end of the beam. First they validated their proposed model by comparing the simulation data with the simulation data of another similar paper[4] They analyzed the effect of electrical

load means what happened by keeping all parameter constant, the electrical load is changed. They presented various graph for various electrical load. The changing of natural frequency for the effect they had discussed. Then they analyzed what happen if the Proof mass dimensions and geometry is changed by keeping remaining parameter and properties constant. They proposed some design on the basis of proof mass geometry and gave the simulation result. They discussed the results briefly. They discussed about the natural frequency changing with respect to various geometry of proof mass [5].

On the basis of this paper this simulation based project is conducted. PZT-A integrated bimorph had designed and some simulation work is performed in comsol multi-physics.

# 2 History:

## 2.1 Discovery and early research:

The pyroelectric effect, where a material generates an electric potential in response to a temperature change, was studied by Carolus Linnaeus and Franz Aepinus in the mid-eighteenth century. Drawing on this knowledge, both René Just Haüy and Antoine César Becquerel posited a relationship between mechanical stress and electric charge; however, experiments by both proved inconclusive [6].

The first demonstration of the direct piezoelectric effect was in 1880, by the brothers Pierre Curie and Jacques Curie. They combined their knowledge of pyroelectricity with their understanding of the underlying crystal structures that gave rise to pyroelectricity to predict crystal behavior, and demonstrated the effect using crystals of tourmaline, quartz, topaz, cane sugar, and Rochelle salt (sodium potassium tartrate tetrahydrate). Quartz and Rochelle salt exhibited the most piezoelectricity [7].

The Curies, however, did not predict the converse piezoelectric effect. The converse effect was mathematically deduced from fundamental thermodynamic principles by Gabriel Lippmann in 1881 [8]. The Curies immediately confirmed the existence of the converse effect, and went on to obtain quantitative proof of the complete reversibility of electro-elasto-mechanical deformations in piezoelectric crystals [9]

For the next few decades, piezoelectricity remained something of a laboratory curiosity. More work was done to explore and define the crystal structures that exhibited piezoelectricity. This culminated in 1910, with the publication of Woldemar Voigt's Lehrbuch der Kristallphysik (textbook on crystal physics), which described the 20 natural crystal classes capable of piezoelectricity, and rigorously defined the piezoelectric constants using tensor analysis [10]

## 2.2 World War I and Post-War:

The first practical application for piezoelectric devices was sonar, first developed during World War I. In France in 1917, Paul Langevin and his coworkers developed an ultrasonic submarine detector. The detector consisted of a transducer, made of thin quartz crystals carefully glued

between two steel plates, and a hydrophone to detect the returned echo. By emitting a high-frequency chirp from the transducer, and measuring the amount of time it takes to hear an echo from the sound waves bouncing off an object, one can calculate the distance to that object [11].

The use of piezoelectricity in sonar, and the success of that project, created intense development interest in piezoelectric devices. Over the next few decades, new piezoelectric materials and new applications for those materials were explored and developed.

Piezoelectric devices found homes in many fields. Ceramic phonograph cartridges simplified player design, were cheap and accurate, and made record players cheaper to maintain and easier to build. The development of the ultrasonic transducer allowed for easy measurement of viscosity and elasticity in fluids and solids, resulting in huge advances in materials research. Ultrasonic time-domain reflectometers (which send an ultrasonic pulse through a material and measure reflections from discontinuities) could find flaws inside cast metal and stone objects, improving structural safety.

## 2.3 World War II and Post-War:

During World War II, independent research groups in the United States, Russia, and Japan discovered a new class of human-made materials, called ferroelectrics, which exhibited piezoelectric constants many times higher than natural materials. This led to intense research to develop barium titanate and later lead zirconate titanate materials with specific properties for particular applications [12].

Development of piezoelectric devices and materials in the United States was kept within the companies doing the development, mostly due to the wartime beginnings of the field, and in the interests of securing profitable patents. New materials were the first to be developed—quartz crystals were the first commercially exploited piezoelectric material, but scientists searched for higher-performance materials [13]. Despite the advances in materials and the maturation of manufacturing processes, the United States market had not grown as quickly. Without many new applications, the growth of the United States' piezoelectric industry suffered.

In contrast, Japanese manufacturers shared their information, quickly overcoming technical and manufacturing challenges and creating new markets. Japanese efforts in materials research created piezoceramic materials competitive to the U.S. materials, but free of expensive patent restrictions. Major Japanese piezoelectric developments include new designs of piezoceramic filters, used in radios and televisions, piezo buzzers and audio transducers that could be connected directly into electronic circuits, and the piezoelectric igniter which generates sparks for small engine ignition systems (and gas-grill lighters) by compressing a ceramic disc. Ultrasonic transducers that could transmit sound waves through air had existed for quite some time, but first saw major commercial use in early television remote controls. These transducers now are mounted on several car models as an echolocation device, helping the driver determine the distance from the rear of the car to any objects that may be in its path.

# 3 Piezoelectricty:

Piezoelectricity, also called the piezoelectric effect, is the ability of certain materials to generate an AC (alternating current) voltage when subjected to mechanical stress or vibration, or to vibrate when subjected to an AC voltage, or both. The most common piezoelectric material is quartz. Certain ceramics, Rochelle salts, and various other solids also exhibit this effect.

## 3.1 Piezoelectric material:

Piezoelectric materials belong to a larger class of materials called ferroelectrics. One of the defining traits of a ferroelectric material is that the molecular structure is oriented such that the material exhibits a local charge separation, known as an electric dipole.

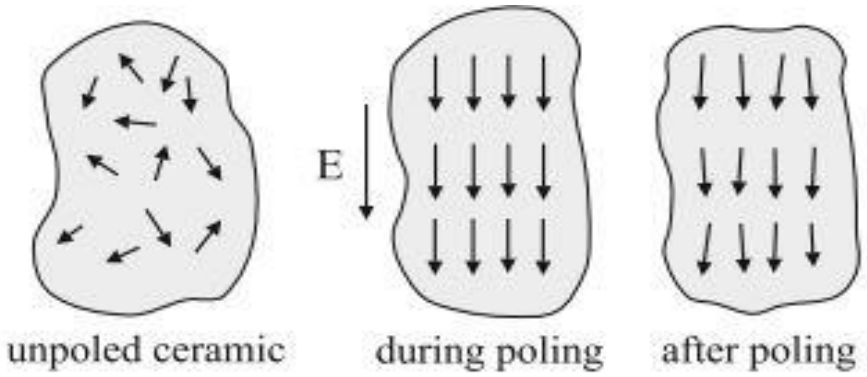


**Figure 1 : Domain structure of ferroelectric materials and their behavior during poling process.**

Throughout the material composition the electric dipoles are orientated randomly, but when the material is heated above a certain point, the Curie temperature, and a very strong electric field is applied, the electric dipoles reorient themselves relative to the electric field; this process is termed poling. Once the material is cooled, the dipoles maintain their orientation and the material is then said to be poled. After the poling process is completed the material will exhibit the piezoelectric effect [14].

Figure 1 shows a typical hysteresis curve created by applying an electric field to a piezoelectric ceramic element until the maximum (saturation) polarization $P_{sat}$ is reached, reducing the field to zero determines the remanent polarization $P_r$ reversing the field attains a negative maximum (saturation) polarization and negative remanent polarization, and re-reversing the field restores the positive remanent polarization.When the electric field is the coercive field $E_c$ there is no net polarization due to the mutual compensation of the polarization of different domain [15].

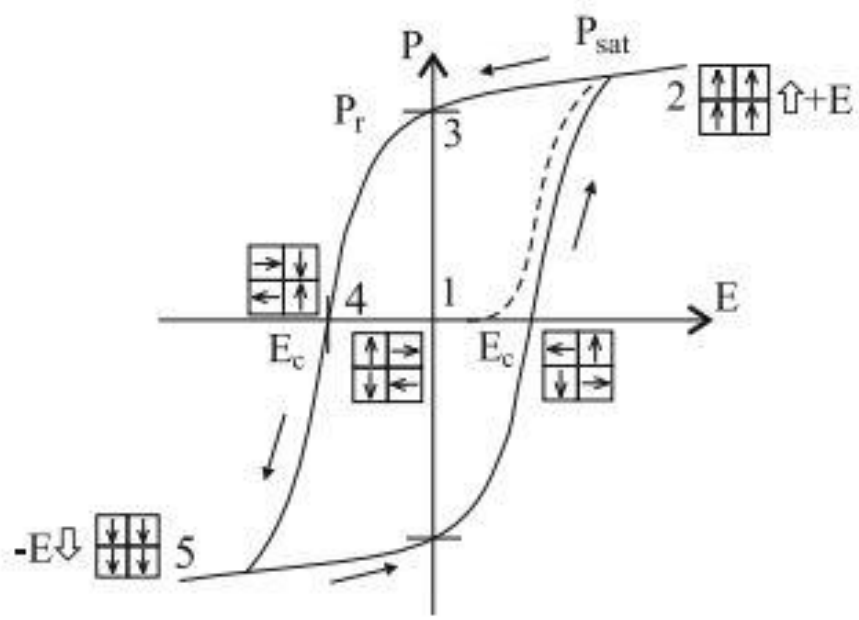


**Figure 2 : Hysteresis curve for polarization of piezoelectric material**

Therefore, the piezoelectric properties must contain a sign convention to facilitate this ability to apply electric potential in three directions. For the sake of keeping this discussion simple, the piezoelectric material can be generalized for two cases. The first is the stack configuration that operates in the –33 mode and the second is the bender, which operates in the –13 mode. The sign convention assumes that the poling direction is always in the "3" direction, with this point the two modes of operation can be understood. In the –33 mode, the electric field is applied in the "3" direction and the material is strained in the poling or "3" direction; in the –31 mode, the electric field is applied in the "3" direction and the material is strained in the "1" direction or perpendicular to the poling direction. These two modes of operation are particularly important when defining the electromechanical coupling coefficient that occurs in two forms: the first is the actuation term d, and the second is the sensor term g. Thus g13 refers to the sensing coefficient for a bending element poled in the "3" direction and strained along "1". It is easy to achieve a certain amount of stress with the'31'-mode by bonding the piezoelectric element to a substructure undergoing bending. In comparison with '33'-mode generators, this is more suitable for MEMS applications. A typical 31-mode power generator is a beam type piezoelectric power generator, in which a piezoelectric layer is bonded to a host element. When the host element is vibrating under the external excitation, a corresponding deformation is induced in the piezoelectric layer.[16]

Piezoelectric effects are mainly two type.one is direct and another is converse. They are described individually below.

## 3.2 Direct Piezoelectric Effect:

The direct piezoelectric effect describes the material's ability to transform mechanical strain into electrical charge The direct piezoelectric effect is responsible for the material's ability to function as a sensor.

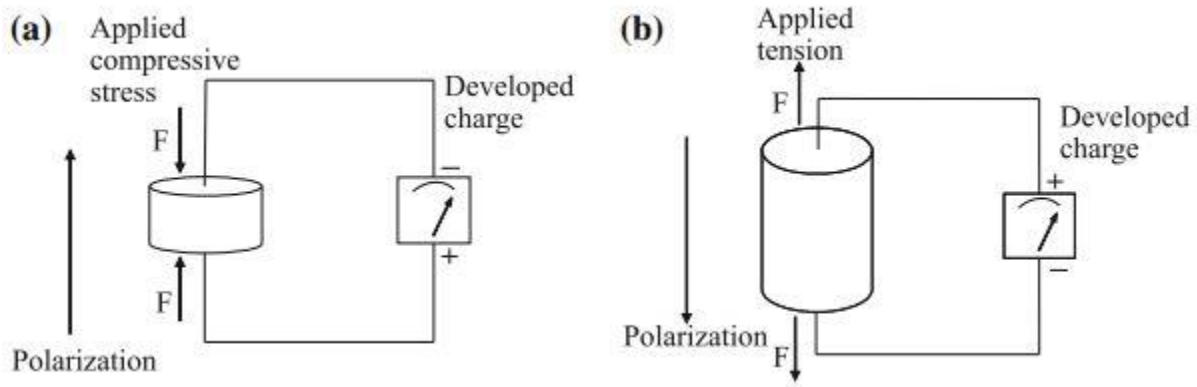


Figure 3 : Direct piezo-effect: a:at applied compressive stress , b:at applied tension

The mechanical and electrical behavior of a piezoelectric material can be modeled by two linearized constitutive equations.[17]

Direct Piezoelectric effect : $\{D\} = [e]^T \{S\} + [\alpha^S] \{E\}$

## 3.3 Converse Piezoelectric Effect :

The second form is the converse effect, which is the ability to convert an applied electrical potential into mechanical strain energy. The converse piezoelectric effect is accountable for its ability to function as an actuator.

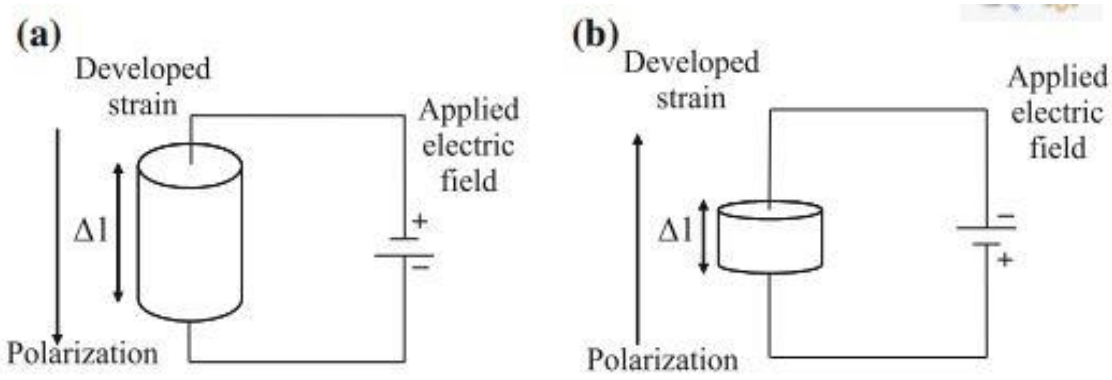


Figure 4: (a) Inverse, (b)converse Piezo-effect at applied electric field

A material is deemed piezoelectric when it has this ability to transform electrical energy into mechanical strain energy, and likewise to transform mechanical strain energy into electrical charge.

$$\text{Converse Piezoelectric effect:} \quad \{T\} = [c^E]\{S\} - [E]\{e\}$$

Here, {D} is the electric displacement vector, {T} is the stress vector, [e] is the dielectric permittivity matrix, $[c^E]$ is the matrix of elastic coefficients at constant electric field strength,{S} is the strain vector, $[\alpha^S]$ is the dielectric matrix at constant mechanical strain, and {E} is the electric field vector. After the material has been poled, an electric field can be applied in order to induce an expansion or contraction of the material. However, the electric field can be applied along any surface of the material, each resulting in a potentially different stress and strain generation. .[18]

## 3.4 Cantilever Piezoelectric Beam as Energy Harvester:

The most popular structures for vibration based piezoelectric power harvesting systems are piezoelectric cantilever (unimorph or bimorph) beams, which are suitable for small amplitude ambient vibration. Most test results available in the literature were obtained for sinusoidal mechanical motion. Cantilever-type energy harvesting devices function most effectively when the excitation frequencies vary in the vicinity of the fundamental resonant frequency of the electromechanical system. Models of distributed-parameter energy harvesting systems were presented in [19], and approaches based on modal analysis were proposed to solve the dynamical response of the electromechanical system. An energy-based formulation of piezoelectric structures is given in [20]. Some simplified analytical models for a cantilever piezoelectric beam energy harvester are available in the literature. However, as pointed out in [21], errors were unfortunately present in deriving the simplified analytical solutions in several published papers. The authors of the current paper also had the opportunity to examine the analytical results published in the literature, and observed that errors and mistakes of a non-typographical nature indeed existed in the earlier works concerning the derivations of analytical solutions for bimorph piezoelectric structures. The timely paper [22] deals with the analytical solution for a bimorph piezoelectric beam energy harvester carrying a symmetrically placed proof mass.

# 4 Proposed Model:

A piezoelectric power harvester consisting of a piezoelectric bimorph beam and a proof mass is sketched in Figure 5. The piezoelectric beam is clamped onto a vibrating base. As the base vibrates, the mechanical energy is converted into electrical energy through the piezoelectric power harvester. In this section, the mechanical (kinetic, strain, and dissipative) energy, the electrical energy, and the electrical work done on a power-consuming resistor are studied and related to a set of electromechanical variables.

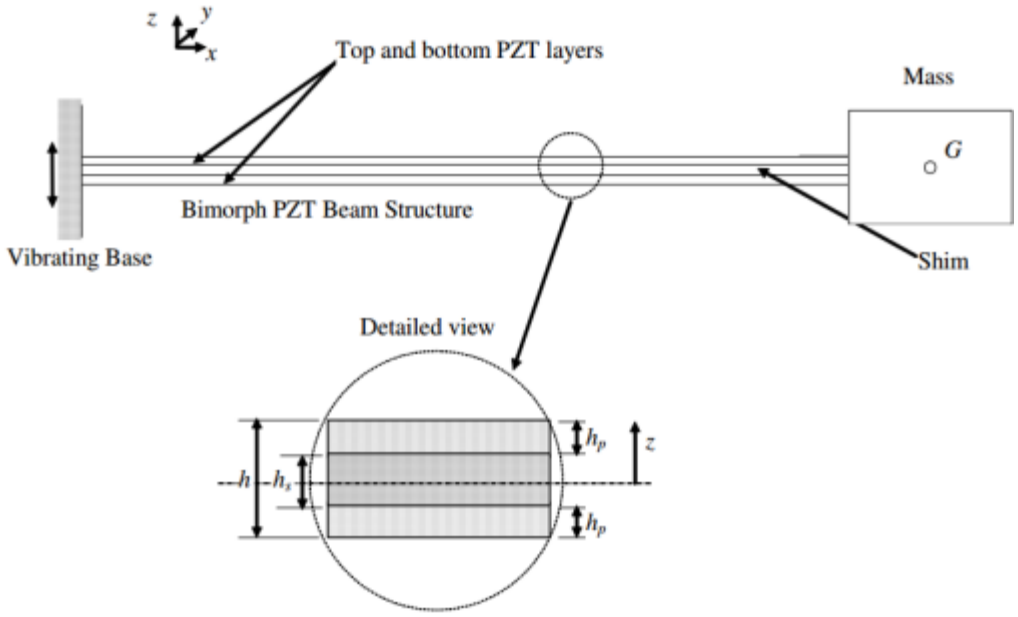


Figure 5: Proposed Model

## 4.1 Theoretical Study of The Beam Bimorph:

### 4.1.1 Axial strain:

The axial strain everywhere in the piezoelectric beam is induced by the axial and lateral deformations in the x -z coordinate plane (see Figure 5). Within the context of classical beam theory, a plane of a beam normal to its neutral axis before deformation remains a plane and normal to the deformed neutral axis after deformation. The total axial displacement of a material point in the beam structure.

bounded by $0 \leq x \leq l$, $-b/2 \leq y \leq b/2$, and $-h/2 \leq z \leq h/2$, may be written as

$$u(x, z, t) = u_0(x, t) - \theta(x, t)z, \tag{1}$$

where u 0.x ;t /is the axial displacement due to uniform axial stretching, w.x ;t /is the lateral displacement of the centroid due to in-plane bending, z is the vertical distance of the material from the centroid, and b is the beam width. According to Euler–Bernoulli beam theory, the angle

of rotation of a beam cross section, normal to the centroid axis, is everywhere related to the slope of the deformed centroid axis as follows:

$$\theta(x,t) = \frac{\partial w(x,t)}{\partial x}, \qquad 0 \le x \le l. \tag{2}$$

For small deformations, the axial strain everywhere in the beam is

$$S_1(x,z,t) = \frac{\partial u_0(x,t)}{\partial x} - \frac{\partial^2 w(x,t)}{\partial x^2} z. \tag{3}$$

where u (x ;t) is the axial displacement due to uniform axial stretching, w(x ,t) is the lateral displacement of the centroid due to in-plane bending, z is the vertical distance of the material from the centroid, and b is the beam width. According to Euler–Bernoulli beam theory, the angle of rotation of a beam cross section, normal to the centroid axis, is everywhere related to the slope of the deformed centroid axis as follows:

### 4.1.2 Constitutive equations:

The constitutive equation for the nonactive shim material,bounded by -hs/2 <z <hs/2,may be written as,

$$T_{1,s} = c_{11,s} S_1, \tag{4}$$

where $T_{1,s}$ is the axial stress in the shim material and $c_{11,s}$ is the modulus of elasticity of the shim material.

For the two piezoelectric layers, bounded by $h_s/2 \le z \le h/2$ and $-h/2 \le z \le -h_s/2$, the constitutive equations may be written as [Roundy et al. 2004]

$$T_{1,p} = c_{11,p} S_1 - e_{31,p} E_{3,p}, \qquad D_{3,p} = e_{31,p} S_1 + \varepsilon_{33,p} E_{3,p}, \tag{5}$$

where $T_{1,p}$ is the axial stress in the piezoelectric material, $C_{11,p}$ is the elastic constant of the piezoelectric material, D3,p is the permittivity in the thickness direction, d 31;p is the piezoelectric constant, $E_{3,p}$ is the electric field in the thickness direction, and $D_{3,p}$ is the electric displacement in the thickness direction. A bimorph piezoelectric beam in the f3-1gmode is made of two identical piezoelectric layers at the top and bottom and a shim in the middle, which makes the structure a symmetrically laminated beam. In a symmetrically laminated beam, the axial stretching does not induce bending, and vice versa. For a composite beam of very large length-to-thickness ratios, the dominating strains and stresses in each constitutive layer are the axial strains and stresses due to the bending and axial stretching when it is operated in the vicinity of the fundamental natural frequency of the in-plane bending. Other stress components, for example the transverse shear stress, are negligible. For piezoelectric composite beams of moderate or large thickness, the electrical field in a piezoelectric layer may vary considerably in the thickness direction [23]. However, for a very thin piezoelectric laminate, the electrical field across each piezoelectric layer may be considered constant in the thickness direction. In this paper, the

piezoelectric structure is thin and symmetric. The following sim-plified relationship between the electric field and the voltage differential .v/ across a single piezoelectric layer is employed:

$$E_{3,p} = \begin{cases} -v/h_p & \text{if } h_s \le 2z \le h, \\ 0 & \text{if } -h_s \le 2z \le h_s, \\ v/h_p & \text{if } -h \le 2z \le -h_s, \end{cases} \quad (6)$$

where hp is the thickness of the top or bottom piezoelectric layer and v is the voltage across one piezo-electric layer

.

### 4.1.3 Motion analysis:

A rigid proof mass is commonly attached to the beam at the free end to enhance power generation. When the beam-mass system is clamped to a rigid moving base, the beam-mass system participates in two motions: the rigid body motion with the base and the elastic motion relative to the base. The rigid reference motion is responsible for providing an excitation in the form of a distributed inertial force field. The relative elastic motion is desired to yield necessary straining of materials for producing electrical charges. A beam-mass system is capable of various types of elastic deformations when the excitation frequencies vary considerably. They include bending, axial stretching/compression, and torsion.

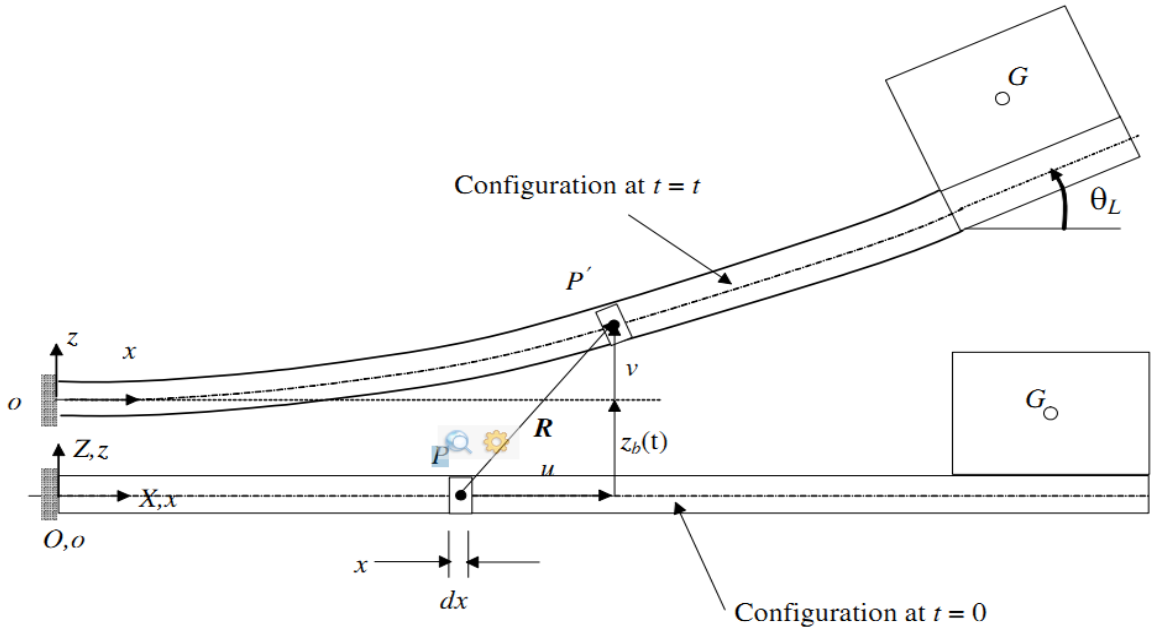


Figure 6 : Mechanics of model

However, when the system is excited in the vicinity of the fundamental natural frequency, the beam motion is predominantly bending in the x -z coordinate plane. The proof mass motion is of the type of general plane motion. Since the lateral motion is coupled to the lateral bending motion for nonsymmetrical attachments of the proof mass, the longitudinal deformation and

lateral bending are considered. Bending in the y –z coordinate plane and torsion about the z axis are negligible. To determine the deformations of a flexible beam at time t, a set of moving coordinates fixed to the moving ground are employed. For translational base motion in the vertical direction, the base-fixed coordinate translates with velocity Pvb . A material point P , located a distance x from the reference point on the neutral axis before deformations, as shown in Figure 2, moves to P 0 after deformations. If the longitudinal and lateral displacements measured with respect to the body-fixed coordinate system x -z are u .x ;t / and w.x ;t /, respectively, the absolute position of P 0 may be written in terms of the base-fixed coordinates as

$$\boldsymbol{R} = \{\boldsymbol{e}_x \;\; \boldsymbol{e}_y\} \begin{Bmatrix} x + u_0(x,t) \\ w_b(t) + w(x,t) \end{Bmatrix}, \tag{7}$$

where Ro is the rigid-body position vector of reference point o , and ex and ey are the two unit vectors of the base-fixed coordinate system. For a nonrotating base motion, these two unit vectors are constant and identical to the unit vectors in the space-fixed coordinates. The velocity of point P 0 may be written in the body-fixed coordinate system as

$$\dot{\boldsymbol{R}} = \{\boldsymbol{e}_x \;\; \boldsymbol{e}_z\} \begin{Bmatrix} \dot{u}_0 \\ \dot{w}_b + \dot{w} \end{Bmatrix}, \tag{8}$$

where Pwb is the velocity of the vibrating base and Pu 0 and Pw are the time rates of longitudinal and lateral deflections with respect to the moving coordinate system.

### 4.1.4 Kinetic energy:

The kinetic energy of the dynamical system may be conveniently written as

$$T = T_{\text{beam}} + T_{\text{mass}}, \tag{9}$$

where Tbeam is the kinetic energy of the beam and Tmass is the kinetic energy of the proof mass plus the portion of the beam bonded to the mass. The kinetic energy of the beam may be written as

$$T_{\text{beam}} = \underbrace{\frac{1}{2}\int_0^l \bar{m}\dot{R}^2 dx}_{\text{translational}} + \underbrace{\frac{1}{2}\int_0^l \bar{i}_y \dot{\theta}^2 dx}_{\text{rotational}}, \tag{10}$$

where Nm is the mass of the beam per unit length, Ni y is the mass moment of inertia of the beam about the y -axis per unit length, and Pis the rate of the angle of rotation of a plane normal to the centroid. For a symmetrically laminated beam of constant width b , we can compute Nm and Ni y by

$$\bar{m} = \sum_{k=1}^{n} \rho_k h_k b, \qquad \bar{i}_y = \frac{1}{3}\sum_{k=1}^{n} \rho_k b\left\{\left(z_2^{(k)}\right)^3 - \left(z_1^{(k)}\right)^3\right\}, \tag{11}$$

where z .k /1 and z .k /2 are the z -coordinates of the lower and upper faces of k -th layer, k is the density of the material in k -th layer, and h k is the thickness of k -th layer. For large length-to-thickness ratios, the rotary inertia of the beam bimorph is very small, and will be ignored in this paper. The kinetic energy of the proof mass attached to the free end of the piezoelectric beam structure may be written as

$$T_{\text{mass}} = \tfrac{1}{2} m[\dot{X}_G^2 + \dot{Z}_G^2] + \tfrac{1}{2} J_{G,y} \dot{\theta}_l^2, \tag{12}$$

where PX G and PZ G are the velocities of the proof mass center along the x and z directions respectively, JG ;y is the mass moment of inertia of the proof mass about the y axis, m is the mass of the proof mass, and Pl is the angle of rotation of the beam at x Dl . At a given instant, the proof mass center is related to the beam deflection as

$$X_G = u_{0,l} + a_G \cos\theta_l - c_G \sin\theta_l, \qquad Y_G = w_b + w_l + a_G \sin\theta_l + c_G \cos\theta_l, \tag{13}$$

where $a_G$ and $c_G$ are the axial and lateral distances, respectively, of proof mass center $(G)$ with reference to the end point of the beam neutral axis at $x = l$, and $u_{0,l}$ and $w_l$ are the axial and lateral deformations of the beam at $x = l$.

Finally, the kinetic energy of the proof mass may be written as

$$T_{\text{mass}} = \tfrac{1}{2} m(\dot{X}_G^2 + \dot{Y}_G^2) + \tfrac{1}{2} J_{G,y} \dot{\theta}_l^2. \tag{14}$$

### 4.1.5 Strain energy:

The strain energy of the composite beam associated with the longitudinal and lateral deformations is

$$\begin{aligned} V &= \frac{1}{2}\int_{V_p} T_{1,p} S_1 \, dV_p + \frac{1}{2}\int_{V_s} T_{1,s} S_1 \, dV_s \\ &= \frac{1}{2}\int_{V_p} c_{11,p} (S_1)^2 dV_p + \frac{1}{2}\int_{V_p} e_{31} h_p^{-1} \upsilon S_1 \, dV_p + \frac{1}{2}\int_{V_s} c_{11,s} (S_1)^2 dV_s, \end{aligned} \tag{15}$$

where $V_s$ is the volume of the shim material and $V_p$ is the volume of the piezoelectric material.

Substituting (3) into (15), the strain energy for the symmetrically laminated composite beam may be expressed in terms of a line integral as

$$V = \frac{1}{2}\int_0^l R_u \left(\frac{\partial u_0}{\partial x}\right)^2 dx + \frac{1}{2}\int_0^l R_w \left(\frac{\partial^2 w}{\partial x^2}\right)^2 dx - \frac{1}{2}\int_0^l \gamma \frac{\partial^2 w}{\partial x^2} \upsilon \, dx, \tag{16}$$

where

$$R_u = 2c_{11,p}2A_p + c_{11,s}A_s, \qquad R_w = c_{11,p}I_p + c_{11,s}I_s, \qquad \gamma = 2e_{31}A_p \bar{z}_p h_p^{-1}, \qquad A_p = \tfrac{1}{2}b(h - h_s),$$
$$A_s = bh_s, \qquad I_p = \tfrac{1}{12}b(h^3 - h_s^3), \qquad I_s = \tfrac{1}{12}bh_s^3, \qquad \bar{z}_p = \tfrac{1}{4}(h + h_s).$$

### 4.1.6 Electrical energy:

The electrical energy in the two layers of piezoelectric material may be written as

$$W_e = \frac{1}{2}\int_{V_p} E_3 D_3 dV = \frac{1}{2}\int_0^l \gamma v \frac{\partial^2 w}{\partial x^2} dx + 2\left(\frac{1}{2}c_0 v^2\right), \tag{17}$$

where $c_0 = \varepsilon_{33} b l h_p^{-1}$.

### 4.1.7 Energy dissipation:

Energy loss in a vibrating piezoelectric structure can be handled mathematically if it is in a form of proportionality damping. The proportionality damping accounts for both the environmental damping due to the viscosity of the surrounding medium and the internal structural damping. Within the context of Lagrange equations, the Rayleigh dissipation function is an effective way of bringing damping into consideration. The energy loss function may be assumed as

$$U = \frac{1}{2}\int_0^l \alpha_u \bar{m} \dot{u}_0^2 dx + \frac{1}{2}\int_0^l \alpha_w \bar{m} \dot{w}^2 dx + \frac{1}{2}\int_0^l \beta_u R_u \left(\frac{\partial \dot{u}_0}{\partial x}\right)^2 dx + \frac{1}{2}\int_0^l \beta_w R_w \left(\frac{\partial^2 \dot{w}}{\partial x^2}\right)^2 dx, \tag{18}$$

where

u , w, u, and w are proportionality constants. Their values are not determined individually. Instead, a combined damping ratio associated with a particular mode is measured and used in simulations for a specific setup.

### 4.1.8 Work done on resistor:

The rate of electrical work done by the resistor per unit voltage is

$$\dot{Q}_R = \begin{cases} -i & \text{for piezoelectric layers in parallel,} \\ -2i & \text{for piezoelectric layers in series,} \end{cases} \tag{19}$$

where $i$ is the current passing through the resistor.

The work done by the resistor per unit voltage is then

$$Q_R = \begin{cases} -q & \text{for piezoelectric layers in parallel,} \\ -2q & \text{for piezoelectric layers in series,} \end{cases} \tag{20}$$

where $q$ is the charge flowing through the resistor.

## 4.2 Governing Equation:

In this section, a finite element procedure for obtaining a set of ordinary differential equations for the piezoelectric power harvesting system is presented.

### 4.2.1 Beam finite elements.

The three-node beam element used in this paper has three axial nodal displace-ments, u e1, u e2, and u e3, three lateral displacements, we1, we2, and we3, and three angles of rotation, e1 , e2 ,and e3 . To facilitate the formation of element matrices, a local axial coordinate originating at the firs tnode of a beam element is used. For a straight beam, the local axial coordinate is related to the body-fixed coordinates by Dx x e1 and 0 l e , where x e1 is the axial coordinate of the first node of element and is the local coordinate for element e . The longitudinal and lateral displacements of a material point within a beam finite element may be determined by the shape function and nodal variables from the equations

$$u_e = [N_1(\xi)][D_1^e]\{q_u^e\}, \quad w_e = [N_2(\xi)][D_2^e]\{q_w^e\}. \tag{21}$$

(see [Yu and Cleghorn 2002]). For convenience in assembly of component equations, the global nodal displacement vector is rearranged in the following manner:

$$\{r\} = \{u_1 \;\; w_1 \;\; \theta_1 \;\; u_2 \;\; w_2 \;\; \theta_2 \;\; \ldots \;\; u_{NN} \;\; w_{NN} \;\; \theta_{NN}\}^T . \tag{22}$$

The longitudinal and lateral nodal displacements are related to the global displacement vector through transformation matrices $[T_u^e]$ and $[T_w^e]$ as follows:

$$\{q_u^e\} = [T_u^e]\{r\}, \quad \{q_w^e\} = [T_w^e]\{r\}. \tag{23}$$

### 4.2.2 Expressions for kinetic, strain, and dissipation and electric energies in nodal displacements:

If N e beam finite elements are used for the piezoelectric structure, the kinetic energy (excluding the rotary inertia), the strain energy, the Rayleigh dissipation energy function, and the electrical energy for the dynamical system may be written in terms of the nodal displacements and the voltage across a single layer of piezoelectric material may be written as

$$\begin{aligned} T &= \tfrac{1}{2}\{\dot{r}\}^T[M]\{\dot{r}\} + \dot{w}_b\{\dot{r}\}^T\{B\} + \tfrac{1}{2}\bar{m}l\dot{w}_b^2, & U &= \tfrac{1}{2}\{\dot{r}\}^T[C]\{\dot{r}\}, \\ V &= \tfrac{1}{2}\{r\}^T[K]\{r\} - \tfrac{1}{2}\gamma v\{r\}^T\{\Theta\}, & W_e &= \tfrac{1}{2}v\{r\}^T\{\Theta\} + 2\left(\tfrac{1}{2}c_0v^2\right), \end{aligned} \tag{24}$$

### 4.2.3 Governing equations.

The Lagrangian for the electromechanical system may now be written as

$$L = T - V + W_e = \tfrac{1}{2}\{\dot{r}\}^T[M]\{\dot{r}\} - \tfrac{1}{2}\{q\}^T[K]\{r\} + \gamma\{r\}^T\{\Theta\}v + 2\left(\tfrac{1}{2}c_0v^2\right). \tag{25}$$

Two sets of governing equations for the electromechanical system can be derived from the following Lagrange equations:

$$\frac{d}{dt}\frac{\partial L}{\partial\{\dot{r}\}^T} + \frac{\partial U}{\partial\{\dot{r}\}^T} - \frac{\partial L}{\partial\{r\}^T} = \mathbf{0}, \qquad \frac{d}{dt}\frac{\partial L}{\partial\dot{v}} - \frac{\partial L}{\partial v} = Q_R. \tag{26}$$

Substituting (25) into (26), the equations of motion of the piezoelectric structure and the equation of the electrical power generation are written as

$$[M]\{\ddot{r}\} + [C]\{\dot{r}\} + [K]\{r\} - \gamma[\Theta]v = -\{B\}\ddot{w}_b, \qquad \gamma[\Theta]^T\{r\} + 2c_0v = Q_R. \tag{27}$$

When the electrical output from the piezoelectric structure is connected to a resistor load and the two piezoelectric layers are connected in parallel, the voltage is related to the rate of charge as $v = R\dot{q}$. Incorporating the above electrical boundary condition and the first relation in (20) into (27), the governing equations for the coupled electromechanical system may be rewritten in terms of the mechanical displacements and the electric charge, for a sinusoidal base motion, $w_b = A\sin(\omega t + \phi)$, as follows:

$$\begin{bmatrix}[M] & \mathbf{0}\\ \mathbf{0} & 0\end{bmatrix}\begin{Bmatrix}\{\ddot{r}\}\\ \ddot{q}\end{Bmatrix} + \begin{bmatrix}[C] & -\gamma R[\Theta]\\ \mathbf{0} & R\end{bmatrix}\begin{Bmatrix}\{\dot{r}\}\\ \dot{q}\end{Bmatrix} + \begin{bmatrix}K & \mathbf{0}\\ [\Theta]^T\frac{\gamma}{2c_0} & \frac{1}{2c_0}\end{bmatrix}\begin{Bmatrix}\{r\}\\ q\end{Bmatrix} = A\omega^2\sin(\omega t+\phi)\begin{Bmatrix}\{B\}\\ 0\end{Bmatrix}. \tag{28}$$

Equation (28) is valid for two piezoelectric layers connected in parallel. The voltages across the two piezoelectric layers are each equal to the voltage across the resistor.In the case where the two piezoelectric layers are connected in series, the voltage across the resistor is twice the voltage across each piezoelectric layer, that is, v DR Pq =2. In the case of a series connection, one obtains the following governing equations for the electromechanical system:

$$\begin{bmatrix}[M] & \mathbf{0}\\ \mathbf{0} & 0\end{bmatrix}\begin{Bmatrix}\{\ddot{r}\}\\ \ddot{q}\end{Bmatrix} + \begin{bmatrix}[C] & -[\Theta]\gamma\frac{R}{2}\\ \mathbf{0} & R\end{bmatrix}\begin{Bmatrix}\{\dot{r}\}\\ \dot{q}\end{Bmatrix} + \begin{bmatrix}K & \mathbf{0}\\ [\Theta]^T\frac{\gamma}{c_0} & \frac{2}{c_0}\end{bmatrix}\begin{Bmatrix}\{r\}\\ q\end{Bmatrix} = A\omega^2\sin(\omega t+\phi)\begin{Bmatrix}\{B\}\\ 0\end{Bmatrix}. \tag{29}$$

### 4.2.4 Handling mechanical boundary conditions.

If the base is considered rigid, the piezoelectric beam is clamped to the base. The axial displacement, the lateral displacement, and the angle of rotation of the beam with respect to the base are zero. The boundary conditions at the clamping end can be easily handled using the elimination method or the penalty method [24]. In this paper, the elimination method is employed. It is noted that other boundary conditions, such as elastically restrained edges simulating less than rigid constraints between the base and the beam, can also be handled in the frame work of the finite element formulation. Deleting the first three equations and the first three

nodal variables in the remaining equations in (28), the governing equations for the electromechanical system, which satisfy all electrical and mechanical boundary conditions for the parallel connection of the two piezoelectric layers, may now be written as

$$\begin{bmatrix} [\tilde{M}] & \mathbf{0} \\ \mathbf{0} & 0 \end{bmatrix} \begin{Bmatrix} \{\ddot{\tilde{r}}\} \\ \ddot{q} \end{Bmatrix} + \begin{bmatrix} [\tilde{C}] & -\gamma R[\tilde{\Theta}] \\ \mathbf{0} & R \end{bmatrix} \begin{Bmatrix} \{\dot{\tilde{r}}\} \\ \dot{q} \end{Bmatrix} + \begin{bmatrix} \tilde{K} & \mathbf{0} \\ [\tilde{\Theta}]^T \frac{\gamma}{2c_0} & \frac{1}{2c_0} \end{bmatrix} \begin{Bmatrix} \{\tilde{r}\} \\ q \end{Bmatrix} = A\omega^2 \sin(\omega t + \phi) \begin{Bmatrix} \{\tilde{B}\} \\ 0 \end{Bmatrix}, \quad (30)$$

where matrices with a tilde on top are the result of their corresponding matrices with the first three rows and columns deleted, and vectors with a tilde are the result of their corresponding vectors with the first three elements deleted. Similarly, Equation (29) for the series connection of the two piezoelectric layers can also be mod- ified to satisfy the boundary condition at the clamped end. The governing equations for the coupled electromechanical system may be written as

$$\begin{bmatrix} [\tilde{M}] & \mathbf{0} \\ \mathbf{0} & 0 \end{bmatrix} \begin{Bmatrix} \{\ddot{\tilde{r}}\} \\ \ddot{q} \end{Bmatrix} + \begin{bmatrix} [\tilde{C}] & -[\tilde{\Theta}]\frac{\gamma R}{2} \\ \mathbf{0} & R \end{bmatrix} \begin{Bmatrix} \{\dot{\tilde{r}}\} \\ \dot{q} \end{Bmatrix} + \begin{bmatrix} \tilde{K} & \mathbf{0} \\ [\tilde{\Theta}]^T \frac{\gamma}{c_0} & \frac{2}{c_0} \end{bmatrix} \begin{Bmatrix} \{\tilde{r}\} \\ q \end{Bmatrix} = A\omega^2 \sin(\omega t + \phi) \begin{Bmatrix} \{\tilde{B}\} \\ 0 \end{Bmatrix}. \quad (31)$$

Equation (30) for the coupled electromechanical system can be written in a unified manner as

$$[M_{\text{em}}]\{\ddot{x}_{\text{em}}\} + [C_{\text{em}}]\{\dot{x}_{\text{em}}\} + [K_{\text{em}}]\{x_{\text{em}}\} = \{F_{\text{em}}\} \sin(\omega t + \phi), \quad (32)$$

where the subscript em in the above equations stands for electromechanical. Other quantities are defined as follows for the two piezoelectric layers in parallel:

$$[M_{\text{em}}] = \begin{bmatrix} [\tilde{M}] & \mathbf{0} \\ \mathbf{0} & 0 \end{bmatrix}, [C_{\text{em}}] = \begin{bmatrix} [\tilde{C}] & -\gamma R[\tilde{\Theta}] \\ \mathbf{0} & R \end{bmatrix}, [K_{\text{em}}] = \begin{bmatrix} \tilde{K} & \mathbf{0} \\ [\tilde{\Theta}]^T \frac{\gamma}{2c_0} & \frac{1}{2c_0} \end{bmatrix}, \{x_{\text{em}}\} = \begin{Bmatrix} \{\tilde{r}\} \\ q \end{Bmatrix}, \{F_{\text{em}}\} = A\omega^2 \begin{Bmatrix} \{\tilde{B}\} \\ 0 \end{Bmatrix}.$$

For the two piezoelectric layers in series, the electromechanical mass matrix and the load vector are iden- tical to those given above. However, the electromechanical damping matrix and the electromechanical stiffness matrix are different and are given as:

$$[C_{\text{em}}] = \begin{bmatrix} [\tilde{C}] & -[\tilde{\Theta}]\frac{\gamma R}{2} \\ \mathbf{0} & R \end{bmatrix}, \qquad [K_{\text{em}}] = \begin{bmatrix} \tilde{K} & \mathbf{0} \\ [\tilde{\Theta}]^T \frac{\gamma}{c_0} & \frac{2}{c_0} \end{bmatrix}.$$

### 4.2.5 Steady-State Solution:

A steady-state solution to (32) may be sought in the following manner:

$$\{x_{\text{em}}\} = \{X\}_c \cos(\omega t + \phi) + \{X\}_s \sin(\omega t + \phi), \tag{33}$$

where $\{X\}_c$ and $\{X\}_s$ are constant vectors.

Substituting (33) into the governing differential equations and comparing the coefficients associated with the cosine and sine harmonics, one obtains the following set of inhomogeneous algebraic equations for the two unknown vectors:

$$\begin{bmatrix} [K_{\text{em}}] - [M_{\text{em}}]\omega^2 & [C_{\text{em}}]\omega \\ -[C_{\text{em}}]\omega & [K_{\text{em}}] - [M_{\text{em}}]\omega^2 \end{bmatrix} \begin{Bmatrix} \{X\}_c \\ \{X\}_s \end{Bmatrix} = \begin{Bmatrix} \mathbf{0} \\ \{F_{\text{em}}\} \end{Bmatrix}. \tag{34}$$

Once fX gc and fX gs are determined, the amplitudes for the mechanical variables (nodal displacements) and the electrical variable can be computed. A post processing scheme can be employed to obtain the amplitudes for the current, voltage and power. It is noted that there are two ways to determine the power output: the peak power and the average power. For the sinusoid ally varying current and voltage across an electrical load, the average power is one half of the peak power. For a piezoelectric system under sinusoidal base motion, (34) can be used to obtain the mechanical and electrical responses provided that the damping ratio accounts for the loss of energy in the form of structural damping. For small scale vibration, the air resistance is negligible.

## 4.3 Equivalent Electrical Circuit:

The two piezoelectric layers are connected in a series manner to power a resistive load. An electrical load of 470 kohm is used. Electrical circuit of the system is given bellow:

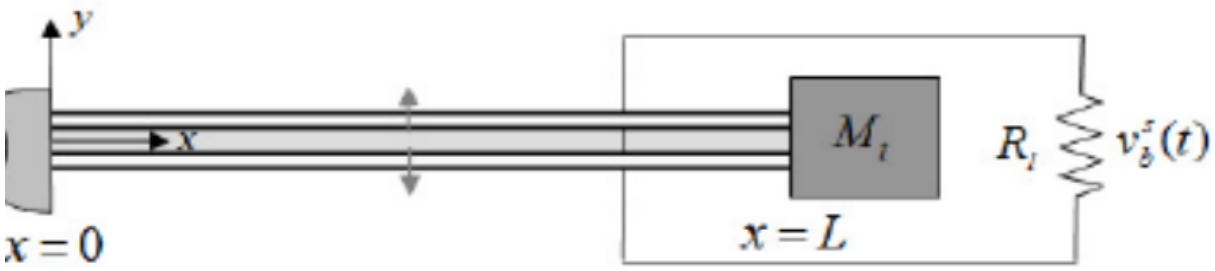


Figure 7 : Equivalent Electrical Circuit

# 5 Simulation:

## 5.1 Construction of the Proposed Model:

The trial model was created using solidworks 2016. Final design was created using comsol. The model is simple a cantilever beam (One end is attached to a fixed support other one is free and can deflect transversely). The cantilever beams material (shim material) is brass and the piezoelectric material is PZT-5A. The PZT-A layer were integrated using glue. The structure constructed using comsol is given below.

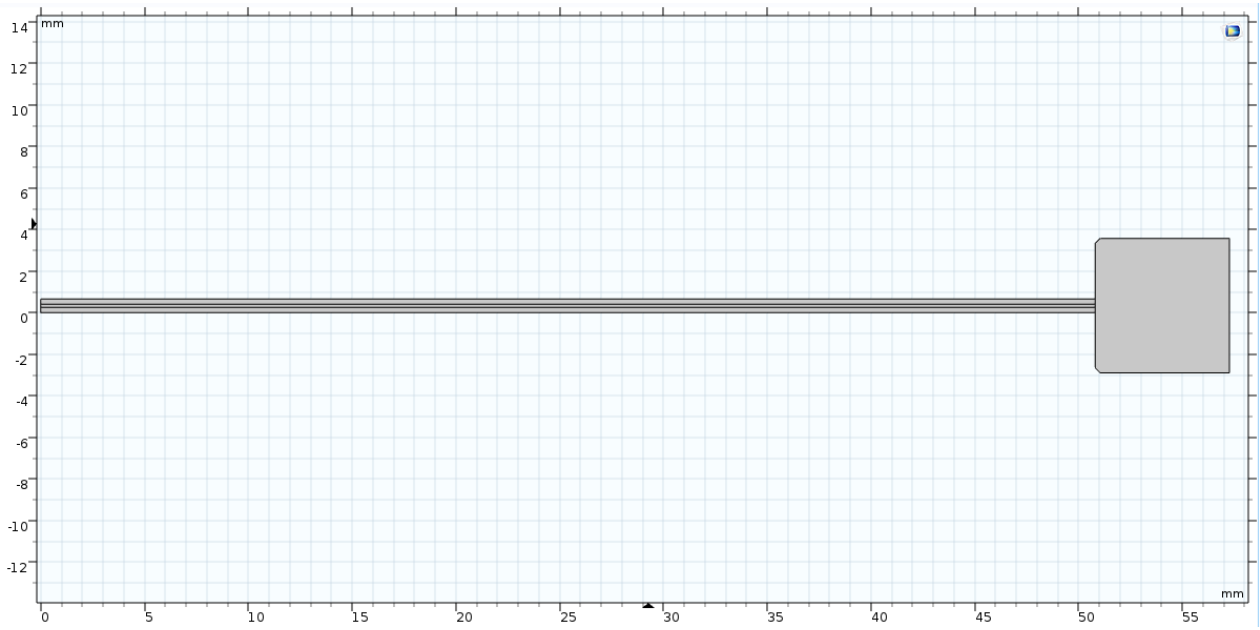


Figure 8 : Bimorph Cantilever Beam

## 5.2 Dimensions and Properties of The structure and Material:

Dimensions of the structure and the properties of those material is given in Table 1.The length, width and other dimensions are chosen from respective paper. Damping ratio is 0.027 and it is taken from experimental result.(experiment conducted by Shudong Yu, Siyuan He and Wen Li ) The point mass is treated as small mass compare to whole structure, and so the mass moment of inertia, the mass center (x and z location) is considered as 0.

Table 1 : Dimensions and properties of the Structure

| Parameters | Symbol | Values |
|---|---|---|
| Piezoelectric structure | | |
| Length (mm) | $l$ | 50.8 |
| Width (mm) | $b$ | 31.8 |
| Damping ratio | $\zeta$ | 0.027 |
| Shim material (brass) | | |
| Thickness (mm) | $t_s$ | 0.14 |
| Modulus of elasticity (GPa) | $E_s$ | 105 |
| Shim density (kg/m$^3$) | $\rho_s$ | 9000 |
| Piezoelectric material (PZT-5A) | | |
| Thickness of each piezoelectric layer (mm) | $t_p$ | 0.26 |
| Modulus of elasticity (GPa) | $E_p$ | 66 |
| Density (kg/m$^3$) | $\rho_p$ | 7800 |
| Piezoelectric constant (pm/V) | $d_{31}$ | 190 |
| Piezolayer permittivity (F/m) | $\varepsilon_{33}$ | $1500\varepsilon_0$ |
| Proof mass | | |
| Mass (g) | $m$ | 12.0 |
| Mass moment of inertia (kg m$^2$) | $J_G$ | 0 |
| Mass center $x$-location (mm) | $a_G$ | 0 |
| Mass center $z$-location (mm) | $c_G$ | 0 |

## 5.3 A cantilever bimorph structure carrying a point mass:

The first system, sketched in Figure 3, is a piezoceramic harvester. The dimensions of the proof mass in the plane of base motion are relatively small and thus it is treated as a point mass. The two piezoelectric layers are connected in a series manner to power a resistive load.The bimorph piezoelectric beam consists of a shim core of brass and two layers of piezoceramic materials. Parameters for the piezoelectric power harvester are given in Table 1 for reference. Harmonic motion applied to the structure and the parameters are given below;

Table 2: Harmonic Motions parameters

| Base motion (harmonic) | | |
|---|---|---|
| Acceleration magnitude ($m/s^2$) | $A$ | 1 g or 9.81 |
| Frequency range for testing (Hz) | $\omega$ or $f$ | 30–70 |

The proof mass is treated as a point mass, that is, the effects of the mass moment of inertia and the mass center offset are ignored. An electrical load of R=470kohm was used.After giving the input the structure was meshed properly for accurate calculation.

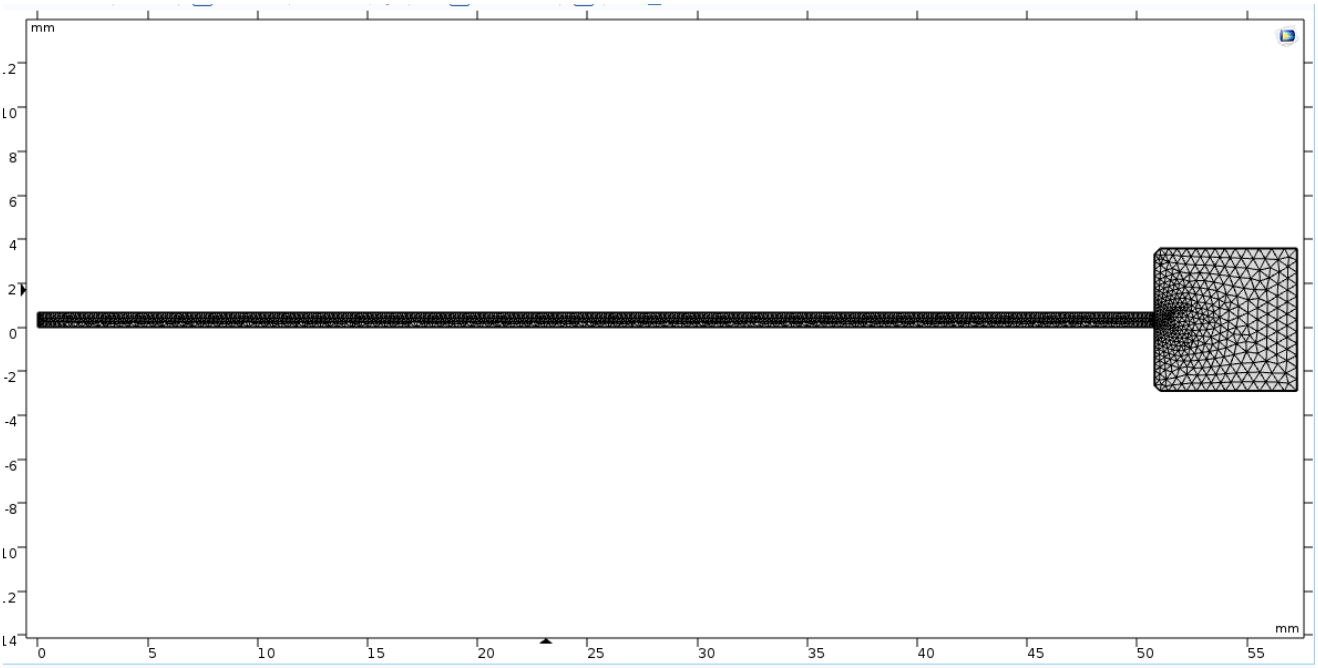


Figure 9 : The Bimorph in Meshed Condition

1g or 9.81m/s$^2$ acceleration was applied in the base of the structure. The motion was harmonic and the frequency range was 30-70Hz. The cantilever beam was in transverse motion and von Mises stress was developed.

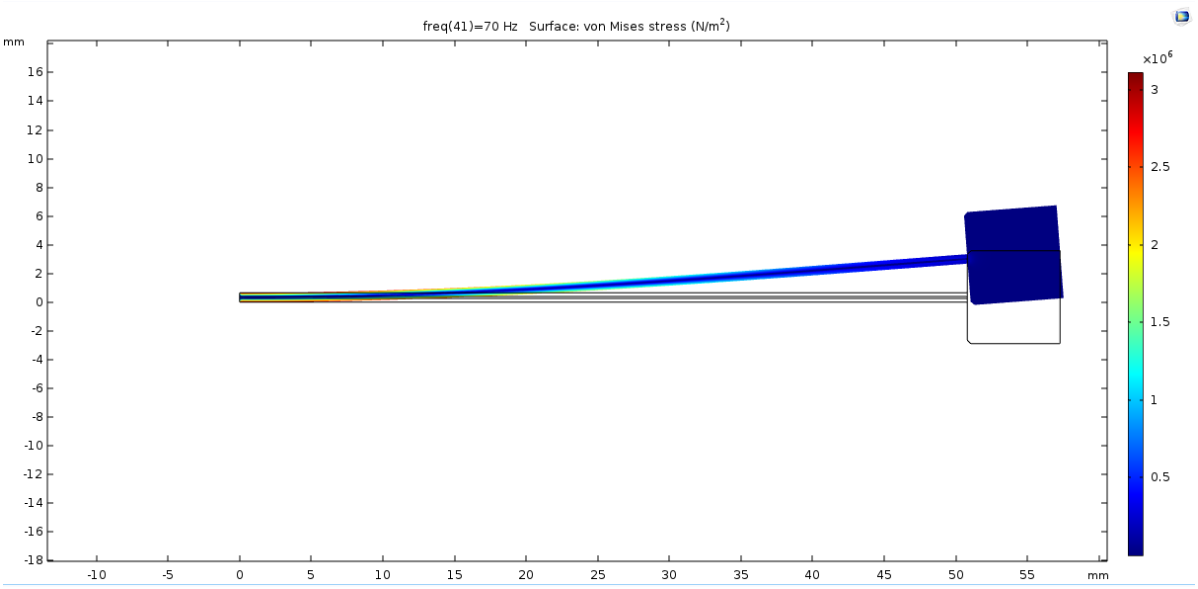


Figure 10 : Surface Von MIses Stess and Deflection of the beam

As the bimorph is deflected, the piezoelectric material will generate electric potential. The Generated electrical potential is showing in the Figure 11.

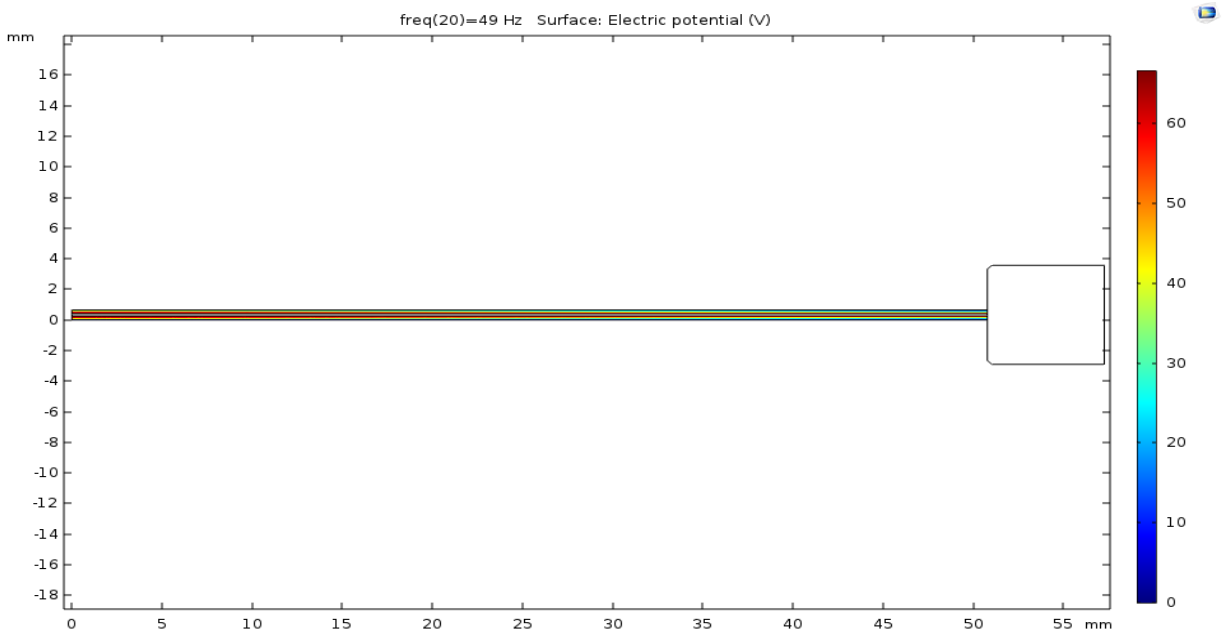


Figure 11 : Surface Electric Potential of the beam

After calculation, the simulation software generate a graph showing input mechanical power, generated voltage and output electrical power.The generated graph is given below.

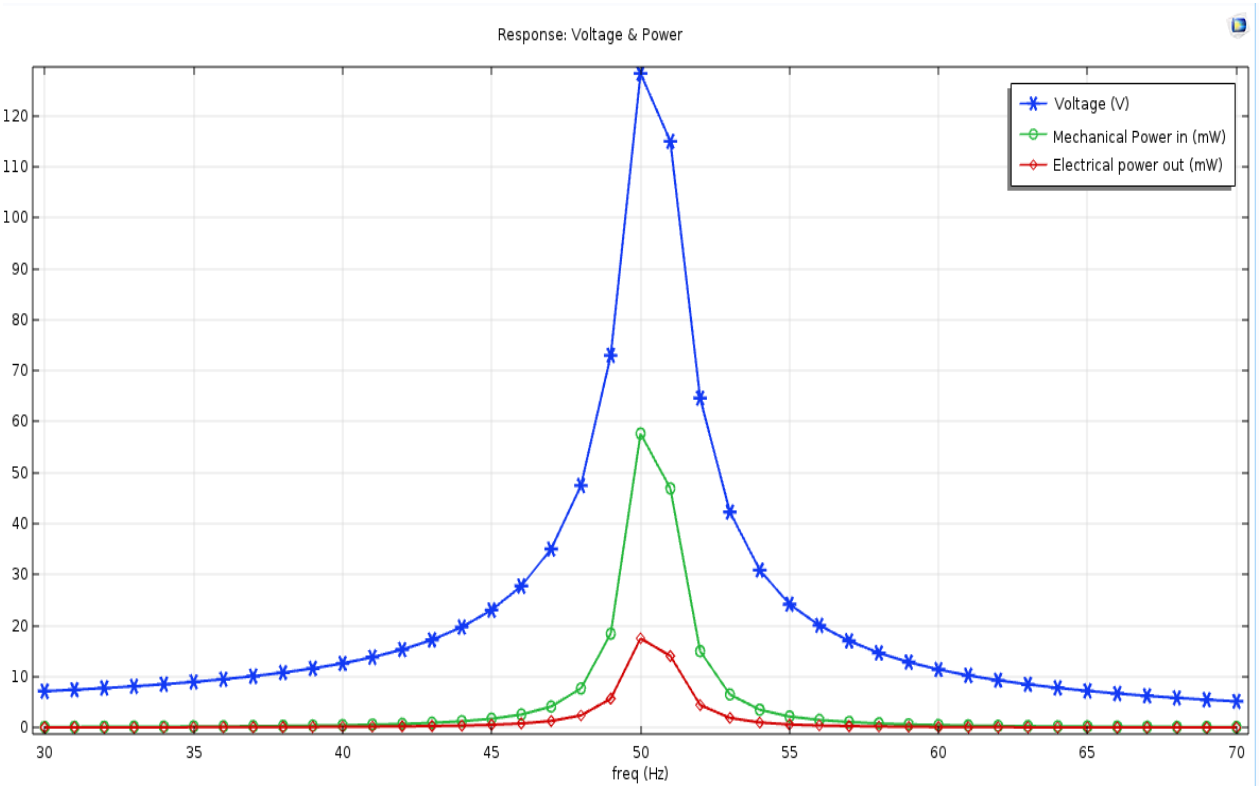


**Figure 12 : Graph showing Voltage , Input and output power**

The peak powers, peak voltages, and optimal frequencies, obtained are given in Table below.

**Table 3 : Simulation result**

| Optimal frequency (Hz) | Input Mechanical power(mW) | Peak voltage (V) | Peak power, Electrical output (mW) |
|---|---|---|---|
| 50 | 57.67 | 123.8 | 17.52 |

Natural frequency = 50Hz

Efficiency = (Output Power)/(Input Power) = (17.52)/(57.67) = 30%

Here the optimal frequencies are the frequencies at which a maximum power (or voltage) is generated for a given resistive load and base excitation amplitude.

## 5.4 Effect of Shim Metals density on Output Power:

Keeping all parameter constant ,how output power is varied if shim materials are changed according to density (ascending order ). 5 materials were chosen for the study.the materials are given in Table 4.

Table 4: Various Metals density and respective power

| Shim Metal | Density(kg/m3) | Output power (mW) |
|---|---|---|
| Aluminum | 2700 | 4.56 |
| Titanium | 4500 | 9.08 |
| Chromium | 6850 | 13.3 |
| Brass | 8400 | 17.52 |
| Lead | 11500 | 29.46 |

In simulation it was observed that theoutpt electrical power was increased as the the density of shi material was increased. Output electrical power vs shim material density graph is plotted .From the graph it is observable that the relation between output power and shim materials density is mostly linear and proportional.

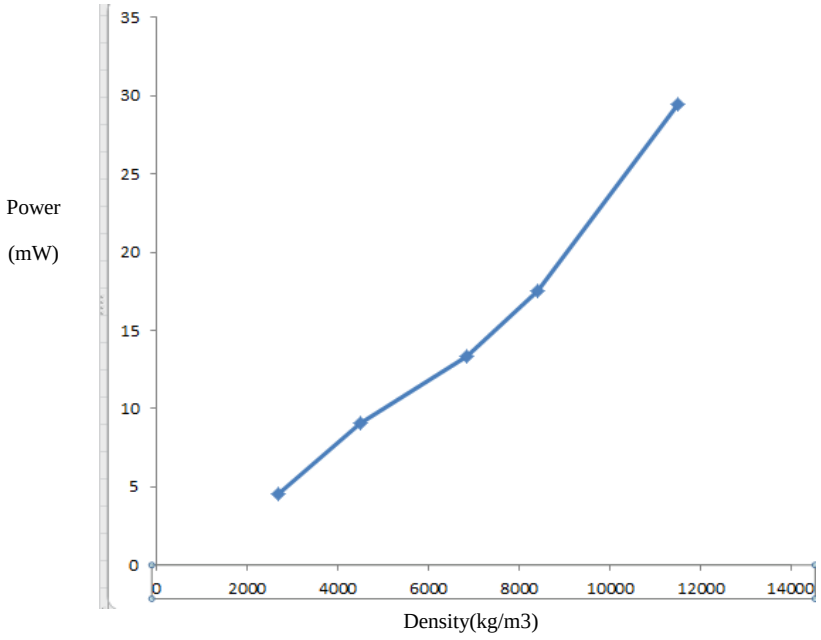


Figure 13 : Graph of Output Power Vs Density

## 5.5 Effect of Proof Mass on Output Power:

The effect of point mass on harvester is studied. 5 different masses were selected for simulation. Except the point mass remaining all parameter were kept same as initial condition.

Table 5 : Output Power for Various Proof Mass

| Proof mass(gm) | Output Power(mw) |
|---|---|
| 6.5 | 10.27 |
| 12 | 17.52 |
| 14.7 | 25.78 |
| 16.7 | 38.4 |
| 21.2 | 51.97 |

For increasing the point mass the output power is proportionally increased. But there is a limitation to increase the point mass. Increasing point mass, once the mass will no longer act as a point mass. (That means the mass moment of inertia and mass center along x and z direction will no longer 0)

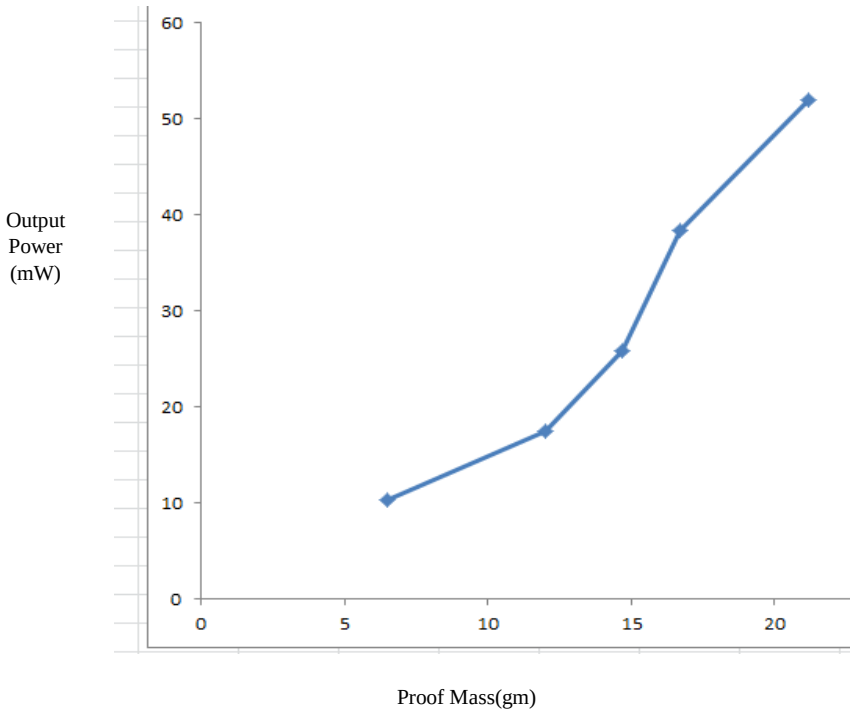


Figure 14: Graph of Output Power Vs Proof Mass

## 5.6 Effect of Beam Width on Output Power:

The relation between width of the structure and output power is studied. For different width of the structure, different power output is generated. As the width of the structure is increased, the output electrical power is also increased.

Table 6 : Output Power for Various width

| Width(mm) | Power(mW) |
|---|---|
| 10 | 7.53 |
| 20 | 13.49 |
| 25 | 15.67 |
| 31.8 | 17.52 |
| 35 | 18.29 |
| 40 | 19.32 |
| 50 | 20.92 |

By plotting a graph Output electrical power vs The width of the structure, it is noticeable that, the output power increase exponentially ,which is represented by the graph.

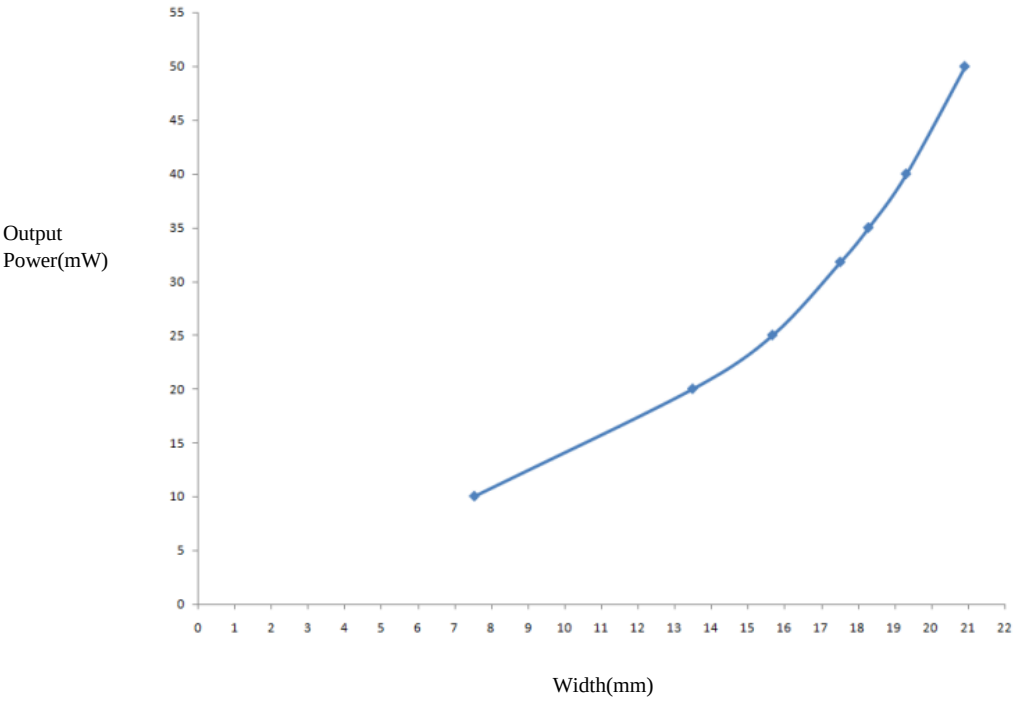


Figure 15 : Graph of Output Power Vs Electrical Lod

## 5.7 Effect of Electrical load on Output Power:

Structures all parameter were kept in initial value, the electric load was changed continuously to observe if any threshold present for this structure. Up to 154kohm of electric load, the output power is increased after that the output power is gradually decreased.

Table 7 : Output Power For Various Electrical Load

| R_load(Kohm) | Power(mW) |
|---|---|
| 100 | 22.81 |
| 125 | 23.69 |
| 140 | 23.906 |
| 145 | 23.942 |
| 150 | 23.96 |
| 153 | 23.964 |
| 154 | 23.965 |
| 155 | 23.964 |
| 157 | 23.962 |
| 160 | 23.955 |
| 165 | 23.937 |
| 170 | 23.902 |
| 175 | 23.86 |
| 200 | 23.53 |
| 300 | 21.34 |
| 400 | 18.99 |
| 500 | 16.94 |
| 600 | 15.22 |

It is noticed that at 154kohm the output power is maximum(23.965mW). At 155kohm the output power started to reduce

As the output power starts to reduce at 155kohm, so this electrical load is threshold For this structure.

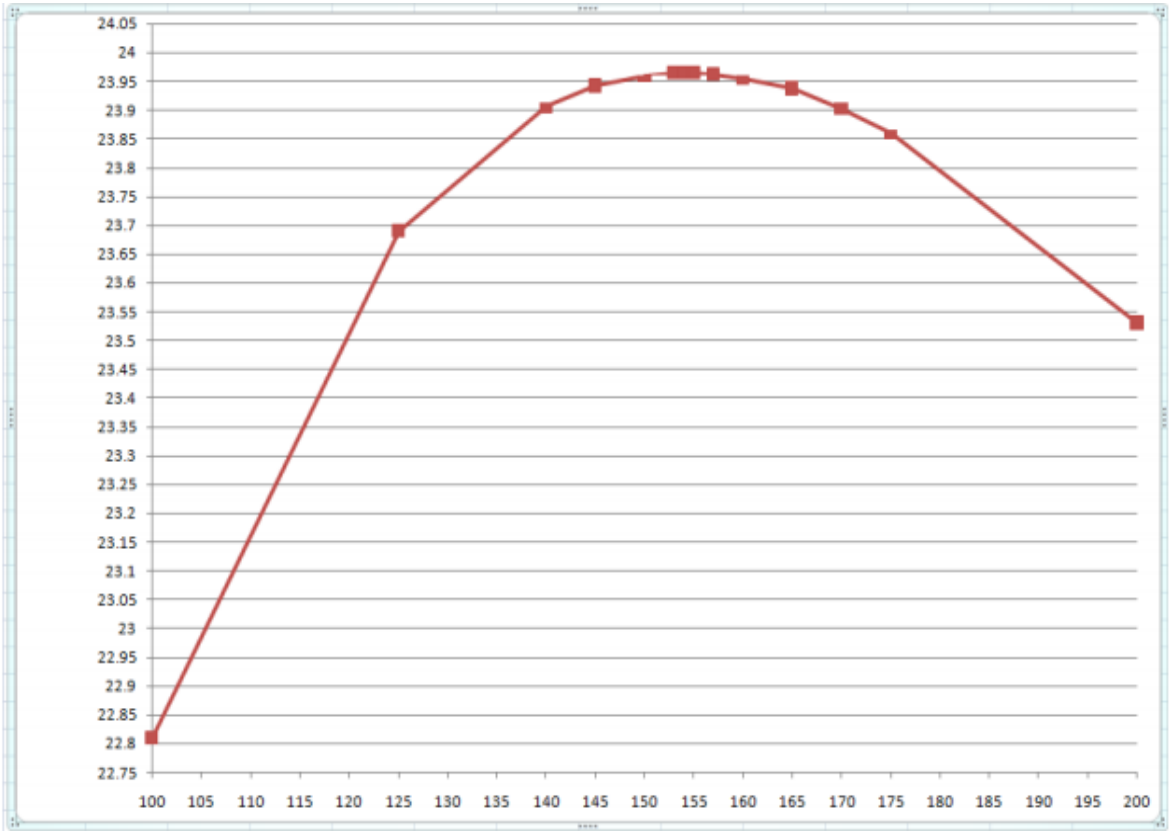


Figure 16 : Graph of Output Power Vs Electrical Load

# 6 Applied Fields of Piezoelectricity:

## 6.1 Energy harvesting in Transport Terminals:

Airport sand railways are vital transportation hubs that will greatly benefit from new energy technologies. Lower costs along with cleaner day-to-day operations from green forms of energy will allow airports to operate more efficiently and effectively. One such idea that will fit well in such setting is the capturing of kinetic energy from passenger foot traffic. This novel idea is not only clean but it is also renewable. Using the floor space in airport terminals allows for a large source of otherwise wasted energy to be captured and utilized as an alternative form of energy for the lighting systems within airports. Placing piezoelectric devices that are used to capture energy from foot traffic underneath airport terminals can effectively capture electrical energy and send it back to the power grid through inverters, which are needed in order to convert the DC power, from the piezoelectric, into AC power used by terminal lighting systems [25].

Other onboard example is the East Japan Railway Company (JR East).It conducted a demonstration experiment from January 19 to March 7, 2008, at Yaesu North Gate, Tokyo Station, on new power-generating floor. Installed at the ticket gate area, it generates electricity from the vibrations created by passengers walking through the ticket gates. The power-generating floor is embedded with piezoelectric elements, which are 35 millimeters in diameter, and disc-shaped components used for loudspeakers. It uses 600 of these elements per square meter. While the loudspeaker creates sound by converting electric signals to vibrations, the floor adopts the reverse mechanism that produces electricity by harnessing the vibrational power generated from passengers' steps. It is being developed by JR East with the aim of making stations more environmentally friendly and energy efficient (Japan for Sustainability, 2008). The piezo devices, due to their small thin shape, could be placed underneath floor tiles or carpet with few complications. In order to harness the power a capacitor could be used to store the electricity like in the train stations or inverters. The power could then be routed directly to specific electrical devices such as lights or billboards or it could be sent to the main power grid in order to supplement the main power supply. There are many installation options and applications of these devices; the specific type of installation will depend upon the intended use of the piezo devices within the terminals. Experimentation with different areas and by observing locations of high foot traffic in such terminals are important in determining the optimal locations for capturing kinetic energy from walking [26].

## 6.2 Energy harvesters in shoes (Moonie Harvesters):

The pressure exerted by a person while walking can converted into electrical energy to power portable devices. This is done by embedding a moonie harvester into a shoe. The "Moonie,' is a metal ceramic composite transducer that has been developed by sandwiching a poled lead zirconate titanate (PZT) ceramic between two specially designed metal end caps. The operating principle of the moonie harvester is also shown in Figure 3. The structure serves as an amplifier for the input force which, in this case, is the weight of the person wearing the shoe. The force on the heel presses the curved plates which in turn expand the piezoelectric disk sandwiched in between the steel plates. The stress is evenly distributed on the disk as opposed to beam structures where the majority of the stress is located at the fixed end of the beam. The energy output of one step was recorded as 81 μJ which translates to 162 μWfor two shoes when walking 2 steps per second. The power density at 1 step / s frequency was measured as 56 μW/cm3. The size of the piezo element was 17.5 mm in diameter and the thickness was 500 μm. The material used was PZT-5H [27].

## 6.3 LPG stove Lighter and Cigarette lighter:

Battery is not required for creating spark. High voltage spark can be generated without any electrical instrument. So for this reason the gas lighter goes not require any other fuel like Butane which is widely used by the common people who use gas lighter for smoking purpose. LPG is now becoming very common in household rather than supplied gas. LPG stove lighter can become a reliable source for people using LPG stoves.

## 6.4 Sensors and actuators:

Piezoelectric material has the ability to convert pressure, strain, and acceleration into electrical emf. Hence the parameters can be measured by means of these materials. Piezoelectric sensors can be used for various purposes. It is used in high precision piezoelectric microphones, electric guitar pickup, strain gauge, pressure sensor, electronic drum pad, accelerometer etc. In piezoelectric actuator converse effect is used. By applying voltage in the material its dimension can be changed, using this concept pressure at micro scale can be provided which cannot be given by hydraulic or pneumatic pressures.

## 6.5 Frequency standard:

Some Piezoelectric material like quartz can vibrate in a defined natural frequency when pulse is applied. It can be of both direct and converse piezoelectric effect. Due to vibration they provide reverse pulse. This mechanism can be used to mark the time and hence can be used as frequency standard.

## 6.6 Sonic and ultrasonic applications:

If a high frequency voltage pulse is applied to a piezoelectric material film it vibrates in a frequency which results in sonic and ultrasonic waves. This can be used for underwater submarine detection, ultrasound in medical technology, metal fault detection etc.

## 6.7 Established Projects:

The energy harvested by the Pavegen tile can immediately power off-grid applications such as pedestrian lighting, way finding solutions and advertising signage or be stored in an onboard battery in the unit. The top surface of the flooring unit is made from 100% recycled rubber and the base of the slab is constructed from over 80% recycled materials. The system is designed can be simply retrofitted in place of existing flooring systems as well specified for new developments. Innowattech[8.9]has developed a new alternative energy system that harvests mechanical energy imparted to roadways, railways and runways from passing vehicles, trains and pedestrian traffic and converts it into green electricity. The system, based on a new breed of piezoelectric generators, harvests energy that ordinarily goes to waste and can be installed without changing the habitat [28].

# 7 Future of Piezoelectricity:

There are two conditions to be satisfied in order to commercialize piezoelectric harvesting. One is that their energy efficiency should improve, and the other is that their prices must go down. The higher piezoelectric element's efficiency gets, the faster and bigger the conversion becomes. Once the technology to improve efficiency at a lower cost is developed, the market will grow much faster. Experts expect the piezoelectric harvesting market to take 28.8% of the entire energy harvesting market soon, as the number of piezoelectric harvesting related projects is increasing rapidly. Piezoelectric harvesting will be considered the next generation energy source as soon as these issues are taken care of.

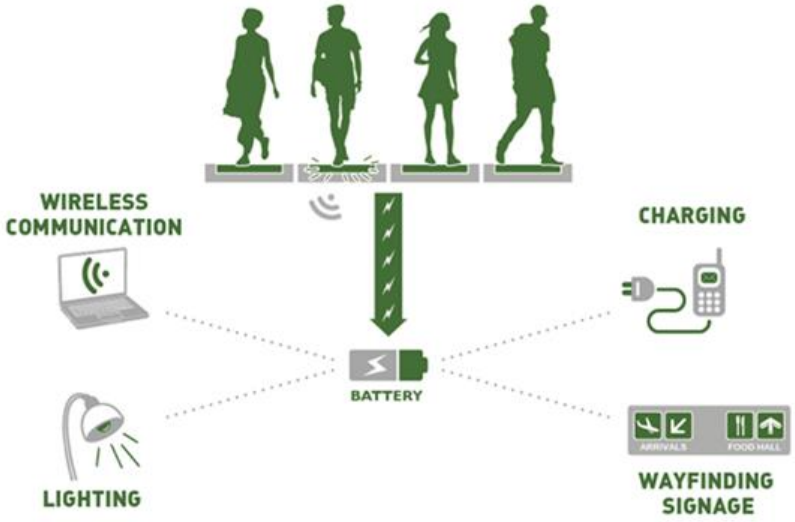


Figure 17 : Piezoelectric harvesting info graphic

Today, we learned about cases in Korea and around the globe related to piezoelectric harvesting as well as their future prospects. The key to 21st century IT is to show the notion of green IT which strives to solve enviro I shared in this posting, there are diverse attempts to advance the green IT market while solving the energy crisis and preventing possible environmental disasters. Though it might sound unfamiliar, energy harvesting is something we can easily find around us. It is important to remember that this eco-friendly technology isn't just an inevitable result of the advancement of IT, but proof of our efforts to find a way to coexist with nature [29].

There are still many environmental issues to solve and countless methods and solutions to be developed in order to do so. I look forward to seeing more green IT that combines nature and technology with insight toward the future rather than simply going for convenience at the moment.

# 8 Conclusion:

A comprehensive model, along with a point mass model, is developed in this paper to simulate the mechanical motion and electrical power of piezoelectric bimorph energy harvesters. The mass moment of inertia and bending-axial stretching coupling effects due to proof mass configuration are considered in the comprehensive model. The simulation results from the point mass and comprehensive models are compared with independent data available in the literature for a series connection between the two PZT layers and newly obtained experimental data for a parallel connection. Excellent agreement was achieved between the theoretical predictions from the comprehensive model and the measurements for both sets of experiments. It is found that the point mass model produces significant errors for both the resonant frequencies and electrical powers. Sensitivity studies conducted using the comprehensive model show that the effects of mass, mass moment inertia, and mass center offset of a proof mass on the electrical power harvesting are significant and must all be taken into consideration in simulations.

# 9 References:


*[1] S. Roundy, P. K. Wright and J. M. Rabaey, Energy scavenging for wireless sensor networks with special focus on vibrations, Kluwer Academic Publishers (2004).*

*[2] Curie J, Curie P (1880a) Développement, par pression, de l'électricité polaire dans les cristaux hémièdres faces ' inclinées. C R Acad Sci Gen 91:294–295*

*[3] Curie J, Curie P (1880b) Sur l'électricité polaire dans les cristaux hémièdres ' faces inclinées. C R Acad Sci Gen 91:383–386*

*[4] Hankel WG (1881) Uber die aktinound piezoelektrischen eigen schaften des bergkrystalles und ihre beziehung zi den thermoelektrischen. Abh Sachs 12:457*

*[5] S. Roundy, P. K. Wright, and J. M. Rabaey, Energy scavenging for wireless sensor networks: with special focus on vibrations, Kluwer Academic Publishers, Boston, 2004.*

*[6] Krautkrämer, J. & Krautkrämer, H. (1990). Ultrasonic Testing of Materials. Springer.[ISBN missing]*

*[7]Erhart, Jiří. "Piezoelectricity and ferroelectricity: Phenomena and propertie"(PDF). Department of Physics, Technical University of Liberec. Archived from the original on May 8, 2014.*

*[8] Curie, Jacques; Curie, Pierre(1880). "Développement par compression de l'électricité polaire dans les cristaux hémièdres à faces inclinées" [Development, via compression, of electric polarization in hemihedral crystals with inclined faces]. Bulletin de la Société minérologique de France. 3: 90–93.*
*Reprinted in: Curie, Jacques; Curie, Pierr (1880). "Développement, par pression, de l'électricité polaire dans les cristaux hémièdres à faces inclinées". Comptes rendus (in French). 91: 294–295.*
*See also: Curie, Jacques; Curie, Pierre(1880). "Sur l'électricité polaire dans les cristaux hémièdres à faces inclinées" [On electric polarization in hemihedral crystals with inclined faces]. Comptes rendus (in French). 91: 383–386.*

*[9] Lippmann, G. (1881). "Principe de la conservation de l'électric" [Principle of the conservation of electricity]. Annales de chimie et de physique (in French). 24: 145.*

*[10] Curie, Jacques; Curie, Pierre(1881). "Contractions et dilatations produites par des tensions dans les cristaux hémièdres à faces inclinées" [Contractions and expansions produced by voltages in hemihedral crystals with inclined faces]. Comptes rendus (in French). 93: 1137–1140.*

*[11] Voigt, Woldemar (1910). Lehrbuch der Kristallphysik. Berlin: B. G. Teubner.*

*[12]Katzir, S. (2012). "Who knew piezoelectricity? Rutherford and Langevin on submarine detection and the invention of sonar" Notes Rec. R. Soc. 66 (2): 141–157. doi10.1098/rsnr.2011.0049*

*[13]M. Birkholz (1995). "Crystal-field induced dipoles in heteropolar crystals – II. physical significanc". Z. Phys. B. 96 (3): 333–
340. Bibcode:1995ZPhyB..96..333B doi:10.1007/BF01313055.*

*[14]U. K. Singh and R. H. Middleton, "Piezoelectric power scavenging of mechanical vibration energy", Australian Mining Technology Conference, 2-4 October (2007), pages 111-118. [15] Roundy S., Wright P. K. and Rabaye J., "A. study of lowlevel vibrations as a power source for wireless sensor nodes", Computer Communications 26 (2003) 1131–1144.*

*[16] Steven R. Anton and Henry A. Sodano, A review of power harvesting using piezoelectric materials (2003-2006), Smart Materials and Structures 16 (2007) R1–R21.*

*[17] Y. C. Shu and I. C. Lien, "Analysis of power output for piezoelectric energy harvesting systems", Smart Materials and Structures 15 (2006), pages 1499-1512.*

*[18] Jan Heine and Andreas Oehler, Vintage Bicycle Press Vol. 3, No. 4, 2005*

*[19] A. Erturk and D. J. Inman, "Issues in mathematical modeling of piezoelectric energy harvesters",*

*[20] N. E. Dutoit, B. L. Wardle, and S.-G. Kim, "Design considerations for MEMS-scale piezoelectric*

*[21] A. Erturk and D. J. Inman, "Comment on 'Modeling and analysis of a bimorph piezoelectric cantilever beam for voltage generation"', Smart Mater. Struct. 17:5 (2008), 058001. Smart Mater. Struct.*

*[22] A. Erturk and D. J. Inman, "An experimentally validated bimorph cantilever model for piezoelectric energy harvesting from base excitations", Smart Mater. Struct. 18:2 (2009), 025009.*

*[23] F. Wang, G. J. Tang, and D. K. Li, "Accurate modeling of a piezoelectric composite beam", Smart Mater. Struct. 16:5 (2007), 1595–1602.*

*[24] K.-J. Bathe, Finite element procedures, 2nd ed., Prentice Hall, Englewood Cliffs, NJ, 1995.mechanical vibration energy harvesters", Integr. Ferroelectr. 71:1 (2005), 121–160.*

*[25] P. Glynne-Jones, M. J. Tudor, S. P. Beeby, and N. M. White, "An electromagnetic, vibration-powered generator for intelligent sensor systems", Sens. Actuators A Phys. 110:1–3 (2004), 344–349.*

*[26] Y. Liao and H. A. Sodano, "Model of a single model energy harvester and properties for optimal power generation", Smart Mater. Struct. 17:6 (2008), 065026.*

*[27] S. Roundy, P. K. Wright, and J. M. Rabaey, Energy scavenging for wireless sensor networks: with special focus on vibrations, Kluwer Academic Publishers, Boston, 2004.*

*[28] H. A. Sodano, G. Park, and D. J. Inman, "A review of power harvesting from vibration using piezoelectric materials", Shock Vib. Digest 36:3 (2004), 197–205.*

*[29] J. Yang, Analysis of piezoelectric devices, World Scientific, Singapore, 2006.*